Preprints of the 19th World Congress
The International Federation of Automatic Control
Cape Town, South Africa. August 24-29, 2014

Real-Time Heave Motion Estimation using Adaptive Filtering Techniques

M. Richter * **K. Schneider** ** **D. Walser** ** **O. Sawodny** *

* *Institute for System Dynamics, University of Stuttgart, P.O. Box 801140, D-70511 Stuttgart, Germany (e-mail: markus.richter@isys.uni-stuttgart.de).*
** *Liebherr Werk Nenzing GmbH, P.O. Box 10, A-6710 Nenzing, Austria.*

Abstract: Active heave compensation (AHC) systems require an accurate estimate of the vertical vessel motion in order to decouple the offshore crane's lift operation from the motion of the vessel. In this work, the heave motion is estimated based on measurements from an inertial measurement unit (IMU) using an adaptive heave filter whose parameters are adapted online. A standard double integrating heave filter introduces large phase errors resulting in large estimation errors for real-time applications. This work presents three modifications of a standard heave filter in order to reduce those phase errors. The error composition of each proposed filter is analyzed. The results are used to derive error functions which are minimized in order to obtain the optimal filter parameters. Furthermore, sea state characteristics, such as the mean heave height and the dominant heave frequency are determined online and utilized for parameter adaptation. The real-time estimation accuracy improves significantly when applying the phase correction algorithms to the filters. This is evaluated using measurement results from the Liebherr AHC test bench.

Keywords: Inertial measurement units; Position estimation; Adaptive filter; Error analysis; Parameter optimization, Noise, Marine systems.

1. INTRODUCTION

Many technical marine applications are based on the knowledge of the vertical motion of the vessel. Safe aircraft landing on vessels (Marconi et al. [2002]) or hydrographic seabed mapping (Work et al. [1998]), where the quality of seabed maps is improved by heave compensation, are only two examples for such marine applications. Another important offshore application is subsea lifting, where heavy loads need to be transferred safely from a vessel to the seabed by an offshore crane which is attached to the vessel. Such lifting operations are necessary for underwater installations like pipelines or conveying systems for oil and gas. Active heave compensation (AHC) systems are supposed to compensate for the vertical vessel motion and thus enable safe crane handling even under harsh sea conditions. However, the AHC system performance strongly depends on the estimation accuracy of the vertical motion.

Due to wave excitation, a vessel moves in six degrees of freedom which can be captured by an inertial measurement unit (IMU). The three accelerometers measure the translational accelerations and the three gyroscopes the rotational angular rates. Since the horizontal motion is usually controlled with dynamic positioning systems, the three dominating directions of a vessel are pitch, roll and heave. In order to obtain position and attitude of a vessel, the accelerometer signals need to be integrated twice and the gyroscope signals once. Due to sensor errors, such as noise and bias, pure integration would result in an infinite drift in position and attitude. Many approaches have been proposed in the literature in order to eliminate this drift. An often used approach is sensor fusion of an IMU and a GPS as presented by Fossen and Perez [2009]. However, this approach strongly depends on the availability of GPS signals. Additionally, GPS performs worst in the vertical direction which is a significant disadvantage for this application.

If not the height (absolute vertical position) but the heave (relative vertical position) is of importance, a standalone IMU is sufficient. The motion is then determined with respect to the current sea level. Thus, tidal changes, for example, cannot be identified with the approaches presented in the following. However, this is not necessary for AHC purposes anyway. Küchler et al. [2011b] propose an observer, implemented as extended Kalman filter, for estimating the heave position with a standalone IMU. The heave motion is approximated by the sum of several overlaying sine waves. Thus, the position can be estimated without any drift. Some approaches make use of a specific hydrodynamic model of the vessel for heave estimation as it is done by Triantafyllou et al. [1983]. Since AHC crane systems are supposed to be independent of the vessel they are attached to, such methods cannot be used for AHC systems. A widely-used approach is the application of a bandpass filter. This filter is a combination of a highpass filter to remove low-frequency components and a double integrator. Such a filter for position estimation is proposed by Godhavn [1998]. He derives an error function which represents the expected mean heave error. The

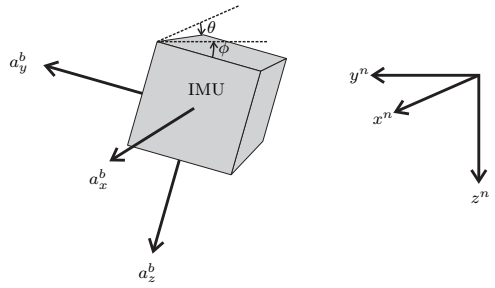

Fig. 1. Rotation of the IMU.

optimal cutoff frequency of the highpass filter is adjusted adaptively to ensure optimal performance. Yang et al. [2009] present a similar approach, evaluating the effect of parameter tuning for heave speed estimation only. Both articles show that the main error for real-time applications results from the phase errors induced by the highpass filter. However, none of the mentioned work focuses on reducing these errors by changing the filter structure, for example.

One of the main contributions of this work is the introduction of several approaches to decrease the phase errors. In addition, all filter parameters are adapted in real-time and optimized according to the derived error functions. As a result, the performance can be improved substantially. The paper is organized as follows. In Section 2, the general concept of heave estimation for AHC systems is described. Subsequently, the underlying error model for the accelerometers is derived before the utilized standard heave filter is presented. Section 3 introduces three different approaches to reduce the filter-induced phase errors by changing the filter structure. Furthermore, error functions for each case are derived in order to determine the optimal filter parameters. The parameters are constantly adapted according to the current sea state which is estimated online. The proposed methods are evaluated and compared in Section 4 using measurement results from a realistic AHC test bench. Concluding remarks are given at the end.

2. HEAVE ESTIMATION

In the following, heave is estimated from the measurements of one IMU. For AHC systems, this IMU needs to be attached to the crane. Thus, it measures accelerations and angular velocities in a local crane-fixed frame which is called the b-frame. Since the heave motion needs to be calculated in a global earth-fixed frame (n-frame), the measurements of the IMU need to be transformed. In Fig. 1, the main rotational directions of the IMU with respect to the n-frame are illustrated. Due to the roll and pitch motions, the IMU is rotated by ϕ about the x-axis and by θ about the y-axis. Not considering these rotations would lead to errors, since the z-axis of the IMU does not point exactly in the direction of gravity or in the direction of the z-axis of the n-frame, respectively. Thus, before the double integration of the z-component can be performed, the accelerometer signals need to be transformed to the n-frame using the rotation matrix $\mathbf{C}_b^n$. The overall signal flow for heave estimation is illustrated in Fig. 2. By using the measured accelerations $\mathbf{a}^b$ and the angular velocities $\boldsymbol{\omega}^b$ in the local b-frame, the attitude of the IMU, respectively the vessel, can be estimated in terms of the Euler-angles ϕ, θ, ψ. The yaw angle ψ cannot

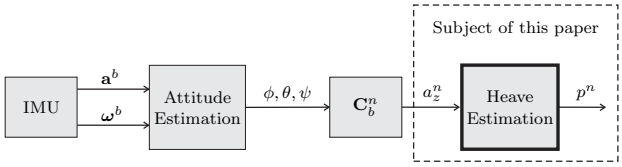

Fig. 2. Block diagram for overall heave estimation.

be calculated exactly without external aid (see Rehbinder and Hu [2004]) such as a magnetometer. However, ψ has no influence on the direction of the vertical axis. Thus, it is sufficient to guarantee that ψ cannot grow infinitely. The z-component of the accelerations can now be used for the actual heave estimation part in order to obtain the heave position. Since the scope of the paper is the actual heave estimation, attitude estimation and the transformation are not considered. For the experimental results, realistic ship motions with superimposed pitch and roll are used. For this reason, an attitude estimation is necessary which is done by a similar approach as presented in Küchler et al. [2011a] and in Kim and Golnaraghi [2004].

2.1 Error Model

In the following, all signals are given in the n-frame, the superscript n is thus omitted for better readability. The measured signal a_z contains not only the actual acceleration $\ddot{p}_z$ but also several error sources which can be described by the error model

$$a_z = (1+\epsilon)\ddot{p}_z + (1+\epsilon)g + b + n + m, \tag{1}$$

where g is the gravitational constant, ϵ is a scale error, b is a bias, n is measurement noise and m is an error caused by the misalignment between the z-axis of the accelerometer and the gravity vector. The scale error can be compensated during calibration of the sensor. The misalignment can be neglected since the transformation from the b-frame to the n-frame already compensates for it. As a result, the simplified error model is

$$a_z = \ddot{p}_z + g + b + n. \tag{2}$$

If the signal a_z is integrated twice without compensation for the error sources, the estimated position and velocity would grow infinitely. Thus, the heave filter needs to fulfill the following requirements:

- Double Integration
- Elimination of the bias $b + g$
- Suppression of the measurement noise n
- Small filter-induced estimation errors
- Reasonable settling time.

2.2 Standard Heave Filter

A straight-forward way to obtain a double integrating filter which removes the constant or slowly time varying bias is a combination of a linear highpass filter and a double integrator. In the following, the standard heave filter as defined by Godhavn [1998] is

$$H(s) = \frac{\hat{p}}{a_z}(s) = \frac{s^2}{(s^2 + 2\zeta\omega_c s + \omega_c^2)^2}, \tag{3}$$

with s being the Laplace variable, ζ the damping coefficient and ω_c the cutoff frequency of the filter. The position estimate is denoted by $\hat{p}$. The damping coefficient

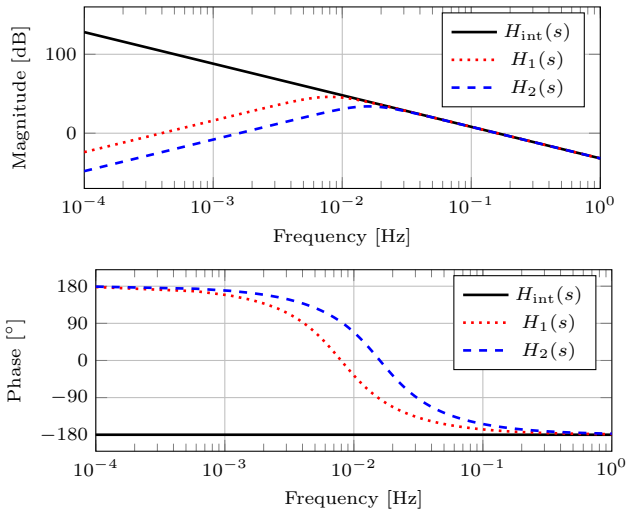

Fig. 3. Bode plot of the transfer functions $H_{\text{int}}(s), H_1(s)$ and $H_2(s)$.

$\zeta = 1/\sqrt{2}$ is chosen in order to obtain the combination of two second order Butterworth filters as highpass filter.

Figure 3 shows the Bode plots of the filters $H_1(s)$ and $H_2(s)$ with the cutoff frequencies $\omega_{c,1} = 0.05\,\text{rad/s}$ and $\omega_{c,2} = 0.1\,\text{rad/s}$ and a double integrator $H_{\text{int}}(s)$. The typical bandwidth of wave motion is between 0.05 Hz and 0.2 Hz. At these frequencies, the filters almost act as double integrators, considering the magnitude response. Thus, the gain errors are very low. Lower frequencies are highly attenuated. The optimal phase for double integration of -180 ° is only reached for frequencies larger than approximately 0.15 Hz. The phase error for lower frequencies leads to a significant error for position estimation. As can be seen in Fig. 3, the errors for phase and magnitude increase with the cutoff frequency. Choosing ω_c very small in order to reduce these errors cannot be done for two reasons: First, the settling time increases with decreasing cutoff frequency. The time constant of the filter is $T = 2\sqrt{2}\pi/\omega_c$, since the step response after a step input Δb, e.g. bias, is given by

$$\begin{aligned}\hat{p} \;=\; & \Delta b\,\frac{t}{2\omega_n}\mathrm{e}^{-\omega_n t}\Big(\cos(\omega_n t)+\sin(\omega_n t)\Big)\\ & -\Delta b\frac{1}{2\omega_n^2}\mathrm{e}^{-\omega_n t}\sin(\omega_n t),\end{aligned} \tag{4}$$

with $\omega_n = \omega_c/\sqrt{2}$. Second, the estimation error induced by measurement noise increases with decreasing cutoff frequency. As a result, the choice of ω_c needs to be a trade-off between reducing the noise-induced errors and the filter-induced errors.

2.3 Error Analysis

The overall heave error can be written as

$$\tilde{p} = p - \hat{p} = \big(1 - s^2 H(s)\big)p - H(s)(g + b + n). \tag{5}$$

Assuming that heave motion can be approximated by wave spectra such as the JONSWAP and the Pierson-Moskowitch spectrum (Chakrabarti [2008]), every wave has one dominant frequency at the point of maximal spectral density function. Thus, for the following error analysis the wave is assumed to be a sinusoid

$$p = A_p \sin(\omega_p t), \tag{6}$$

with amplitude A_p and dominant frequency ω_p. The relative magnitude error for the filter (3) is then given by

$$\begin{aligned} e = ||1 - s^2 H(s)|| \;&\overset{s=i\omega_p}{=}\; \frac{\sqrt{\omega_c^8 + 8\omega_p^6\omega_c^2}}{\omega_p^4 + \omega_c^4}\\ &\to 2\sqrt{2}\,\frac{\omega_c}{\omega_p},\ \text{for } \omega_p \gg \omega_c. \end{aligned} \tag{7}$$

As can be seen in Fig. 3, the largest portion of this error is due to the phase error.

In addition to the deterministic errors, particularly the stochastic errors provoked by the sensor noise are relevant. Assuming that the sensor noise n is white Gaussian noise with variance σ_n^2 and spectral density

$$S_{nn}(\omega) = \sigma_n^2, \tag{8}$$

the variance of the noise induced error is given by

$$\begin{aligned}\sigma_{\tilde{p}_n}^2 &= \frac{1}{2\pi}\int_{\omega=-\infty}^{\infty} S_{\tilde{p}\tilde{p}}(\omega)d\omega\\ &= \frac{1}{2\pi i}\int_{s=-i\infty}^{i\infty} H(s)H(-s)S_{nn}(s)ds.\end{aligned} \tag{9}$$

The variance can be determined analytically using a Phillips-Integral (see Maybeck [1982]) as

$$\sigma_{\tilde{p}_n}^2 = \frac{\sigma_n^2}{2^{7/2}\omega_c^3}. \tag{10}$$

2.4 Optimization and Adaptive Tuning

In order to obtain the best filter performance, the optimal cutoff frequency ω_c, which minimizes the total error resulting from stochastic and deterministic errors, needs to be determined. Thus, the variance of the total estimation error is used as error function which can be approximated by

$$\begin{aligned}\sigma_{\tilde{p}}^2 &= \mathrm{E}[\tilde{p}^2(t)] = \mathrm{E}[(e\,p(t))^2] + \sigma_{\tilde{p}_n}^2\\ &\le 8A_p^2\left(\frac{\omega_c}{\omega_p}\right)^2 + \frac{\sigma_n^2}{2^{7/2}\omega_c^3} = J.\end{aligned} \tag{11}$$

The minimum of this function can be calculated analytically as

$$\omega_{c,\text{opt}} = \frac{1}{2^{3/2}}\left(\frac{3\sigma_n^2\omega_p^2}{A_p^2}\right)^{1/5}. \tag{12}$$

It can be assumed that the sensor noise is constant during operation. However, the sea state and thus the dominant wave frequency and amplitude can change significantly. Therefore, the optimal cutoff frequency changes depending on ω_p and A_p. For this reason, both parameters are determined in real-time by frequency analysis. Using a real-time fast Fourier transform (FFT), the dominant wave frequency can be determined. The mean wave hight A_p can generally be expressed as

$$A_p = \lim_{T\to\infty}\sqrt{\frac{2}{T}\int_0^T p(t)^2 dt}. \tag{13}$$

Considering $p(t) = -a(t)/\omega_p^2$, the mean wave height can be approximated using n buffered values a_j of the acceleration signal a_z from

$$A_p = \sqrt{\frac{2}{N}\sum_{j=0}^{N}\frac{a_j^2}{\omega_p^4}}. \tag{14}$$

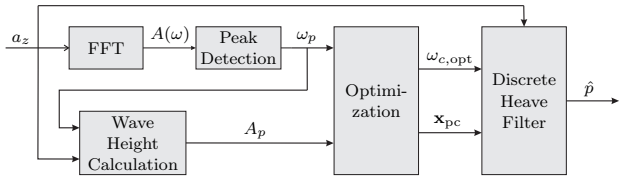

Fig. 4. Signal flow of the adaptive algorithms where all variables are time-varying.

The general signal flow of the proposed adaptive algorithms is illustrated in Fig. 4. The FFT of the acceleration signal a_z is used to obtain the dominant frequency ω_p. The peak detection block also handles special cases such as calm sea or situations where the frequency spectrum contains two or more dominant frequencies. Using different error functions, which are derived in the next section, the optimal filter cutoff frequency $\omega_{c,\mathrm{opt}}$ and the optimal phase correction filter parameters $\mathbf{x}_{\mathrm{pc}}$ are calculated. Then, the discrete heave filter with real-time adapted parameters estimates the position by using the acceleration measurements a_z. It has to be stated that the resulting filter is nonlinear due to changes in parameters. However, the sea state changes slowly and thus the parameter changes are much slower than the dynamic behavior of the actual heave motion. This is farther ensured by a strong lowpass filtering of the determined parameters. The robustness of the implemented algorithms has been confirmed by extensive tests.

3. PHASE CORRECTION ALGORITHMS

As shown in the last section, the largest drawback of a double integrating highpass filter is the phase error which results in large estimation errors. This section presents three different approaches reducing this error in order to improve the real-time estimation performance. Minimizing error functions leads to optimal parameters for the cutoff frequency and optimal values for the phase correction filter parameters.

3.1 Lead-Lag Element

One way to influence the phase response without changing the magnitude response is an allpass filter. The aim is to completely eliminate the overall real-time estimation error for one specific frequency. However, an allpass filter cannot completely eliminate the total error since it only affects the phase. Thus, a lead-lag element $H_{\phi,\mathrm{ll}}$ with two design parameters v and w is added in series to the standard heave filter. The resulting filter is given by

$$H_{\mathrm{ll}} = \frac{s^2}{(s^2+2\zeta\omega_c s+\omega_c^2)^2}\underbrace{\frac{vs+vw}{s+vw}}_{H_{\phi,\mathrm{ll}}}. \tag{15}$$

The lead-lag element is supposed to almost act as an allpass filter while it slightly influences the magnitude in order to completely eliminate the error. The real-time estimation error of this filter is

$$e_{\mathrm{ll}} = ||1-s^2H_{\mathrm{ll}}(s)|| \overset{s=i\omega_p}{=} \frac{||\alpha(\omega_p)+\beta(\omega_p)i||}{(\omega_p^4+\omega_c^4)\sqrt{\omega_p^2+(vw)^2}} \tag{16}$$

with

$$\alpha(\omega_p) = 2\sqrt{2}\omega_c\omega_p^4 - (2\sqrt{2}\omega_c^3+4\omega_c^2vw)\omega_p^2 + vw\omega_c^4, \tag{17}$$

$$\beta(\omega_p) = (1-v)\omega_p^5 - (2\sqrt{2}\omega_cvw+4\omega_c^2)\omega_p^3 + (2\sqrt{2}\omega_c^3vw+\omega_c^4)\omega_p. \tag{18}$$

The real time error disappears if $\alpha(\omega_p)=\beta(\omega_p)=0$. This is the case for

$$v = \frac{\omega_c^6+2\omega_c^2\omega_p^4}{\omega_p^4(\omega_c^2-4\omega_p^2)} - 1, \tag{19}$$

$$w = 2\sqrt{2}\,\omega_p^6\,\frac{\omega_c^2-\omega_p^2}{\omega_c^7+\omega_c^3\omega_p^4+4\omega_c\omega_p^6}. \tag{20}$$

The Bode plots of the standard heave filter $H(s)$, the lead-lag heave filter H_{ll} and the later presented heave filters with a cutoff frequency of $\omega_c = 0.08\,\mathrm{rad/s}$ are shown in Fig. 5. For the calculation of the phase correction parameters v and w a wave period of $\omega_p = 0.63\,\mathrm{rad/s}$, i.e. $f_p = 0.1\,\mathrm{Hz}$, is used. As expected, the magnitude response is almost the same as for the standard heave filter $H(s)$. The phase is lowered to match -180 ° at 0.1 Hz. Unfortunately, the phase error increases in particular for frequencies larger than the estimated dominant wave frequency. Nevertheless, the overall phase error for the typical bandwidth of heave frequencies is reduced significantly. Since the magnitude response remains almost unchanged, the earlier defined error function J can be utilized. In fact, the filter-induced error at frequency ω_p equals zero. However, there is an error for larger and smaller frequencies which can be assumed to be proportional to the original error. Thus, an error scale factor R is introduced, that describes the real-time error improvement by phase correction. As a result, the error function is given by

$$J_{ll} = 8R^2A_p^2\left(\frac{\omega_c}{\omega_p}\right)^2 + \frac{\sigma_n^2}{2^{7/2}\omega_c^3} \tag{21}$$

which leads to the optimal cutoff frequency being

$$\omega_{c,\mathrm{opt,ll}} = \frac{1}{2^{3/2}}\left(\frac{3\sigma_n^2\omega_p^2}{R^2A_p^2}\right)^{1/5}. \tag{22}$$

3.2 Zero Displacement

By simply changing the phase response of the filter, the real-time error can only be eliminated at the dominant heave frequency. At adjacent frequencies (especially larger frequencies), the error is even larger than using the standard heave filter. Another possibility to influence the phase response in a positive way is to displace one of the zeros of the filter. The resulting filter can be written as

$$H_{\mathrm{zd}} = \frac{s(s+a)}{(s^2+2\zeta\omega_cs+\omega_c^2)^2}, \tag{23}$$

where the parameter a needs to be chosen such that the real-time heave error, which is

$$e_{\mathrm{zd}}(a) = \frac{\sqrt{\omega_c^8+8\omega_c^2\omega_p^6+a^2\omega_p^6+4\sqrt{2}\omega_c\omega_p^4a(\omega_c^2-\omega_p^2)}}{\omega_c^4+\omega_p^4}, \tag{24}$$

becomes minimal. The optimal parameter a_{opt} can be determined analytically as

$$a_{\mathrm{opt}} = 2\sqrt{2}\,\omega_c\Big(\frac{\omega_p^6-\omega_c^2\omega_p^4}{\omega_p^6}\Big), \quad \to 2\sqrt{2}\,\omega_c, \text{ for } \omega_p \gg \omega_c. \tag{25}$$

Thus, the minimal real-time heave error is given by

$$e_{\mathrm{zd}}(a_{\mathrm{opt}}) = \frac{\omega_c^2\sqrt{\omega_c^4+16\omega_p^4}}{\omega_c^4+\omega_p^4}, \\ \rightarrow 4\Big(\frac{\omega_c}{\omega_p}\Big)^2, \text{ for } \omega_p \gg \omega_c. \tag{26}$$

Using (9) and a Phillips-Integral yields the noise-induced error of filter $H_{\mathrm{zd}}(s)$, i.e.

$$\sigma^2_{\tilde{p}_n,\mathrm{zd}} = \frac{9}{16}\sqrt{2}\frac{\sigma_n^2}{\omega_c^3}, \tag{27}$$

which is approximately nine times higher than the noise induced error of the standard filter. By minimizing the error function

$$J_{\mathrm{zd}} = 16A_p^2\Big(\frac{\omega_c}{\omega_p}\Big)^4 + \frac{9}{16}\sqrt{2}\,\frac{\sigma_n^2}{\omega_c^3}, \tag{28}$$

the optimal cutoff frequency

$$\omega_{c,\mathrm{opt,zd}} = \Big(\frac{27/1024\sqrt{2}\;\sigma_n^2\omega_p^4}{A_p^2}\Big)^{1/7} \tag{29}$$

can be obtained.

Figure 5 shows the Bode plot of filter $H_{\mathrm{zd}}(s)$. The phase error is almost completely removed for typical heave frequencies. However, the magnitude response has larger errors. Furthermore, the zero displacement filter attenuates low frequency components less than the standard filter.

3.3 Pole-Zero Placement

Another possibility to lower the phase within the required frequency band is to add an additional pole and zero to the transfer function. However, the magnitude is influenced as well with this approach. For this reason, the proposed heave filter has an additional parameter K in order to influence the magnitude response. The transfer function of the filter is given by

$$H_{\mathrm{pz}}(s) = \frac{s^2}{(s^2+2\zeta\omega_c s+\omega_c^2)^2}\;K\;\frac{s-z}{s-p}, \tag{30}$$

with the pole $s_1 = p$ and the zero $n_1 = z$. The optimal parameters p, z, K and ω_c are obtained by constrained minimization of the error function

$$J_{\mathrm{pz}} = A_p^2\big(Q_1 e_{\mathrm{pz}}(\omega_p) + Q_2 e_{\mathrm{pz}}(\omega_{p,2}) + Q_3 e_{\mathrm{pz}}(\omega_{p,3})\big) \\ + (Q_1+Q_2+Q_3)\,\sigma^2_{\tilde{p}_n,\mathrm{pz}}(z,p,K,\omega_c), \tag{31}$$

where $\sigma^2_{\tilde{p}_n,\mathrm{pz}}$ denotes the noise induced error depending on the filter parameters. The proposed error function does not only contain the error at one specific frequency ω_p but penalizes the errors at two adjacent frequencies $\omega_{p,2}$ and $\omega_{p,3}$ as well. With the parameters Q_1, Q_2 and Q_3, the different errors can be weighted. As a result, the estimation error can be minimized within a realistic frequency band for heave motion instead of one dominant frequency only. The adjacent frequencies are chosen to be proportional to the dominant frequency with $\omega_{p,2} < \omega_p$ and $\omega_{p,3} > \omega_p$. Additionally, constraints need to be considered in order to obtain a stable filter with acceptable settling time. It has to be mentioned that the constrained optimization does not necessarily have to be executed in real-time. The optimal parameters depending on ω_p, A_p and σ_n^2 can be calculated offline and stored in lookup tables.
The Bode plot of filter (30) with a fixed cutoff frequency

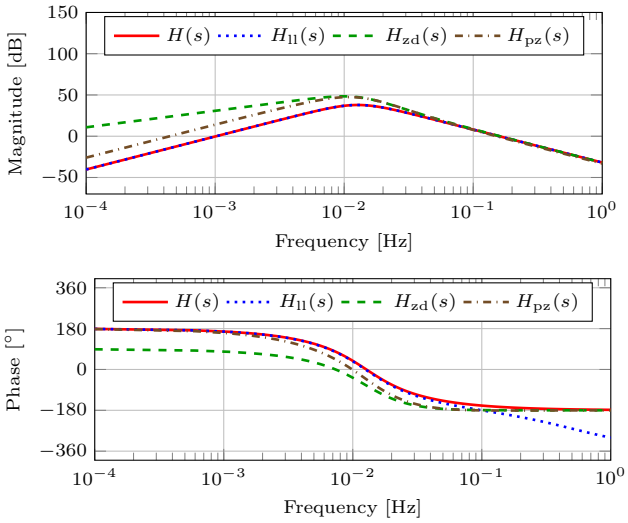

Fig. 5. Bode plot of the transfer functions $H(s), H_{\mathrm{ll}}(s)$, $H_{\mathrm{zd}}(s)$ and $H_{\mathrm{pz}}(s)$ with fixed cutoff frequency $\omega_c = 0.08\,\mathrm{rad/s}$. The phase correction parameters are calculated using $A_p = 1\,\mathrm{m}$ and $\omega_p = 0.63\,\mathrm{rad/s}$.

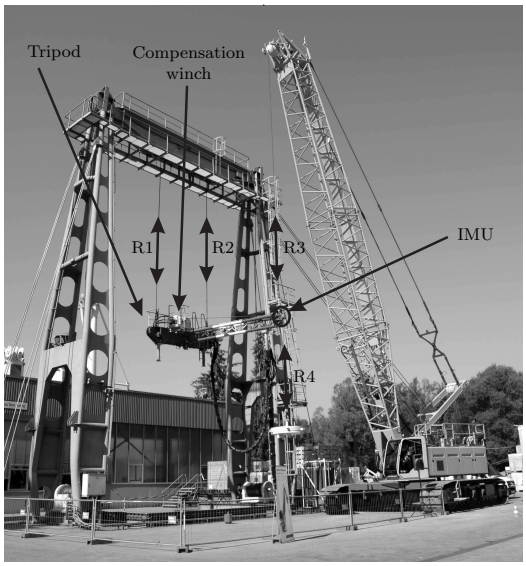

Fig. 6. Liebherr AHC test bench.

of $\omega_c = 0.08\,\mathrm{rad/s}$ is shown in Fig. 5. Filter $H_{\mathrm{pz}}(s)$ removes the phase error almost completely. Similar to the zero displacement approach, the magnitude response errors increase. However, especially the low frequency components are attenuated better. For this reason, the noise-induced error is reduced by approximately 25% on average in comparison to filter $H_{\mathrm{zd}}(s)$.

4. EXPERIMENTAL RESULTS

Figure 6 shows the test bench used to compare the proposed heave filters during an experiment. The body in the middle of Fig. 6, called Tripod, can be moved by three ropes (R1, R2 and R3) that are actuated by hydraulic winches. This allows for imitation of the three dominant motions of a vessel, namely, heave, pitch and roll. The accelerations and angular velocities are measured by an IMU which is attached to the tip of the Tripod. In order

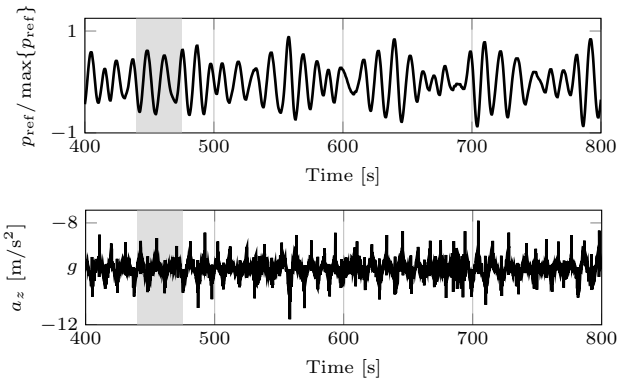

Fig. 7. Normalized reference position p_{ref} of the Tripod (top) and the measured acceleration a_z (bottom) during the experiment. The time range for Fig. 8 is shaded gray.

to compensate for its motion and to keep the load at a fixed position, the winch located on the Tripod can be used. As this contribution only focuses on heave estimation, the compensation winch is not actuated during the experiment. Furthermore, as mentioned earlier, to obtain the vertical acceleration required for position estimation, the measurements need to be transformed to the n-frame (see Fig. 2). This is done using a similar algorithm as presented in Küchler et al. [2011a] and in Kim and Golnaraghi [2004]. Therefore, only the transformed acceleration a_z is considered in the following. The performance of the heave filters can be evaluated using rope length R3, which is measured by an incremental encoder, as a reference.

For the presented experiment, the Tripod is excited by a simulated vessel motion for heave, pitch and roll. Thereby, the motion sequence is obtained from a 6 DOF simulation of a vessel using the Marine Systems Simulator (MSS [2013]). The vessel was excited by a JONSWAP spectrum with a significant wave height of 6 m and a dominant frequency of 0.63 rad/s. The top plot of Fig. 7 shows the reference position p_{ref} of the Tripod's tip measured by the incremental encoder during the experiment. It is displayed using a normalized plot, where the measured signal is divided by the maximum value during the experiment. The plot below depicts the vertical acceleration a_z measured by the IMU and transformed to the n-frame. It clearly illustrates that the acceleration signal is composed of the heave acceleration, the earth's gravity, some sensor noise and a small sensor bias. Both plots only show a section of the experiment. During the experiment, the position of the Tripod was estimated online by the four previously presented adaptive heave filters. The noise variance σ_n^2 is chosen according to the data sheet of the IMU. The same value is used for all algorithms. For all filters, the mean wave height and the dominant wave frequency are calculated online. The filter parameters are calculated and adapted in real-time utilizing the error functions derived in Sec. 3. This naturally leads to different average cutoff frequencies for each filter. For example, optimal performance of the lead-lag filter in comparison to the zero displacement filter is reached at a significantly lower cutoff frequency. This is due to the significantly smaller influence from sensor noise of the lead-lag filter.

Table 1. Error numbers for the different heave filters. The values are given as percentages of the error when using the standard heave filter.

Error	$H(s)$	$H_{\text{ll}}(s)$	$H_{\text{zd}}(s)$	$H_{\text{pz}}(s)$
RMS [%]	100	55.6	59.6	43.4
MAX [%]	100	59.1	66.4	49.7

Figure 8 only depicts a small time range of the experiment in order to be able to visualize the differences in position estimation. This range is shaded gray in Fig. 7. Yet, this small section is representative for the overall experiment. At the top left, the result using the standard heave filter is presented. As expected, the estimated position has a significant positive phase error. For the other three cases, phase correction is applied. As can be seen at the top right, the lead-lag filter can reduce the error significantly. However, the phase of the heave motion is not perfectly matched. Since the phase is simply corrected at one specific frequency, large phase errors can occur especially when high frequencies are present. At the bottom left, the result using the zero displacement filter is shown. The phase error, especially in the reverse points, is almost zero which confirms the design of this filter. However, large amplitude errors occur which are due to the lower attenuation of sensor noise and filter-induced amplitude errors. The optimized filter using pole-zero placement yields the best result. The estimated position is in very good accordance with its reference regarding phase and amplitude.

To confirm the observations that were made from Fig. 8, error numbers for the complete experiment are calculated and displayed in Tab. 1. The calculation of the error numbers starts after the filter's settling time. For a better comparability, the error numbers are given as percentages of the error when using the standard heave filter. Thus, the error numbers of the standard heave filter are set to 100 %. Two types of errors are considered, the root mean square error and the maximal error of the deviation between reference and estimated position. Table 1 clearly shows that the heave estimation errors can be reduced by more than 50 % using the pole-zero placement filter. The insertion of a lead-lag element as well as the zero displacement method improve the performance of the heave filter by approximately 40 %. Note that the relative performance of the heave filters is strongly dependent on the quality of the acceleration measurements. For example, the lead-lag heave filter attenuates sensor noise much better than the zero displacement filter. Thus, the lead-lag filter is preferable in the case of high sensor noise. However, if the sensor noise is very low, the zero displacement and the pole-zero placement filter have advantages since they introduce a very small filter-induced error. Yet, it can be stated that the proposed phase correction methods, in general, significantly improve the performance of double integrating heave filters. Thus, the presented algorithms contribute to the aim of improving position estimation for AHC systems.

5. CONCLUSION

This paper has presented different approaches for estimating the heave motion of a vessel using measurements of an IMU. Since standard double integrating heave filters

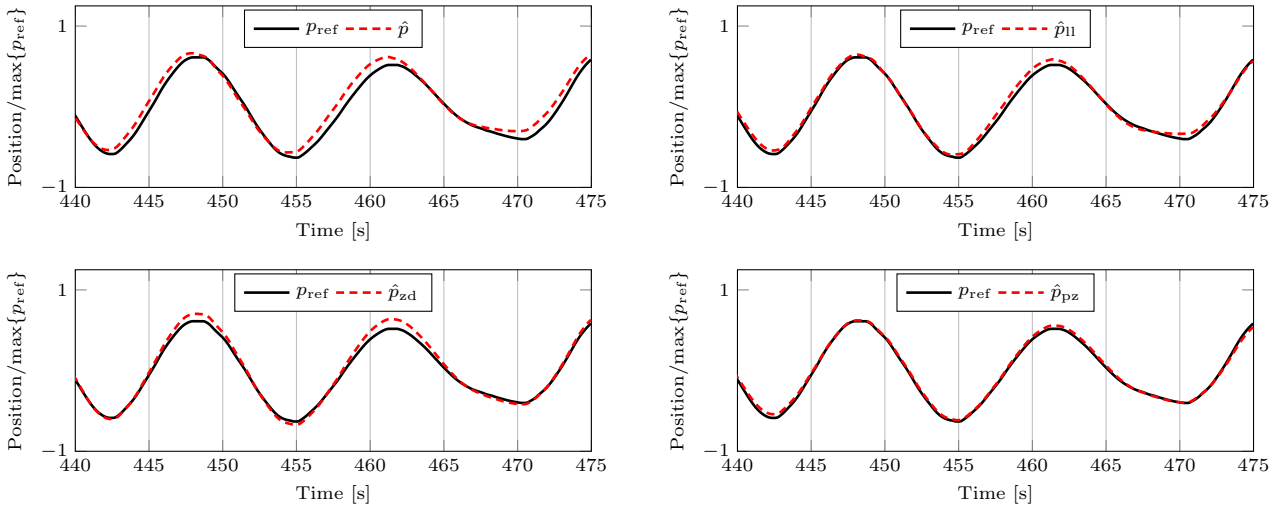

Fig. 8. Normalized reference positions p_{ref} (black, solid) and estimated positions $\hat{p}$ (red, dashed) for the four different adaptive heave filters $H(s), H_{\text{ll}}(s)$, $H_{\text{zd}}(s)$ and $H_{\text{pz}}(s)$.

show large phase errors for real-time applications, three phase corrections methods for reducing these errors were proposed. An error analysis for each filter was performed in order to derive error functions which are minimized to obtain the optimal parameters for each filter. Furthermore, sea state characteristics were calculated online and also used for determining the optimal parameters. Using measurement results from the Liebherr AHC test bench, the proposed methods were validated and compared. The results showed that the performance of position estimation can be improved significantly by applying phase correction. The pole-zero placement approach yields the best results reducing the error by approximately 60 %. Since the performance of AHC systems is strongly dependent on the performance of position estimation, this contribution can obviously help to improve the overall performance of AHC systems. In the future, the presented methods will be incorporated into a complete AHC framework which will be tested at the Liebherr AHC test bench as well.

REFERENCES

S. K. Chakrabarti. *Handbook of Offshore Engineering*. Elsevier, Amsterdam, 2 edition, 2008.

T. I. Fossen and T. Perez. Kalman filtering for positioning and heading control of ships and offshore rigs. *IEEE Control Systems*, 29(6):32–46, 2009.

J.-M. Godhavn. Adaptive tuning of heave filter in motion sensor. In *OCEANS '98 Conference Proceedings*, volume 1, pages 174–178, 1998.

A. Kim and M. F. Golnaraghi. A quaternion-based orientation estimation algorithm using an inertial measurement unit. In *Position Location and Navigation Symposium*, pages 268–272, 2004.

S. Küchler, J. K. Eberharter, K. Langer, K. Schneider, and O. Sawodny. Heave motion estimation of a vessel using accelerometer measurements. In *Proceedings of the 18th IFAC World Congress*, pages 14742–14747, August 2011a.

S. Küchler, C. Pregizer, J. K. Eberharter, K. Schneider, and O. Sawodny. Real-time estimation of a ship's attitude. In *American Control Conference (ACC)*, pages 2411–2416, 2011b.

L. Marconi, A. Isidori, and A. Serrani. Autonomous vertical landing on an oscillating platform: an internal-model based approach. *Automatica*, 38(1):21 – 32, 2002.

P. S. Maybeck. *Stochastic models, Estimation and Control*. Academic Press, 1982.

MSS. Marine System Simulator. www.marinecontrol.org, 2013. Viewed: 06.09.2013.

H. Rehbinder and X. Hu. Drift-free attitude estimation for accelerated rigid bodies. *Automatica*, 40(4):653 – 659, 2004.

M. S. Triantafyllou, M. Bodson, and M. Athans. Real time estimation of ship motions using kalman filtering techniques. *Oceanic Engineering, IEEE Journal of*, 8 (1):9–20, 1983.

P. Work, M. Hansen, and W. Rogers. Bathymetric surveying with GPS and heave, pitch, and roll compensation. *Journal of Surveying Engineering*, 124(2):73–90, 1998.

W. Yang, S. Wei, Z. Zhang, and A. Zhang. Numerical simulation and testing analysis of adaptive heave motion measurements. In *International Conference on Measuring Technology and Mechatronics Automation*, volume 2, pages 263–266, 2009.